NASA/CR-1998-208021

MEASUREMENT AND INTERPRETATION OF CRUSTAL DEFORMATION RATES ASSOCIATED WITH POSTGLACIAL REBOUND

Grant NAG5-1930

Final Report

For the Period 15 March 1992 through 14 March 1998

Principal Investigator

Dr. James L. Davis

May 1998

Prepared for

National Aeronautics and Space Administration
Washington, D.C.

Smithsonian Institution
Astrophysical Observatory
Cambridge, Massachusetts 02138

The Smithsonian Astrophysical Observatory is a member of the Harvard-Smithsonian Center for Astrophysics

The NASA Technical Officer for this grant is Dr. Clark Wilson, Code YS, NASA Headquarters, 300 E. Street, NW, Washington, D.C. 20546

I. Results

This project involves obtaining GPS measurements in Scandinavia, and using the measurements to estimate the viscosity profile of the Earth's mantle and to correct tide-gauge measurements for the rebound effect. Many aspects of this project have been reported in the literature (see Section III). In Section II, we report on the primary geodetic results from this project.

II. Geodetic results

The BIFROST GPS networks (Figure 1) are composed of the permanent GPS networks of Sweden (SWEPOS) and Finland (FinnNet). These networks are described separately below. We then describe the methods used to analyze the GPS phase data, and present an analysis of the errors in our determination of position and velocity.

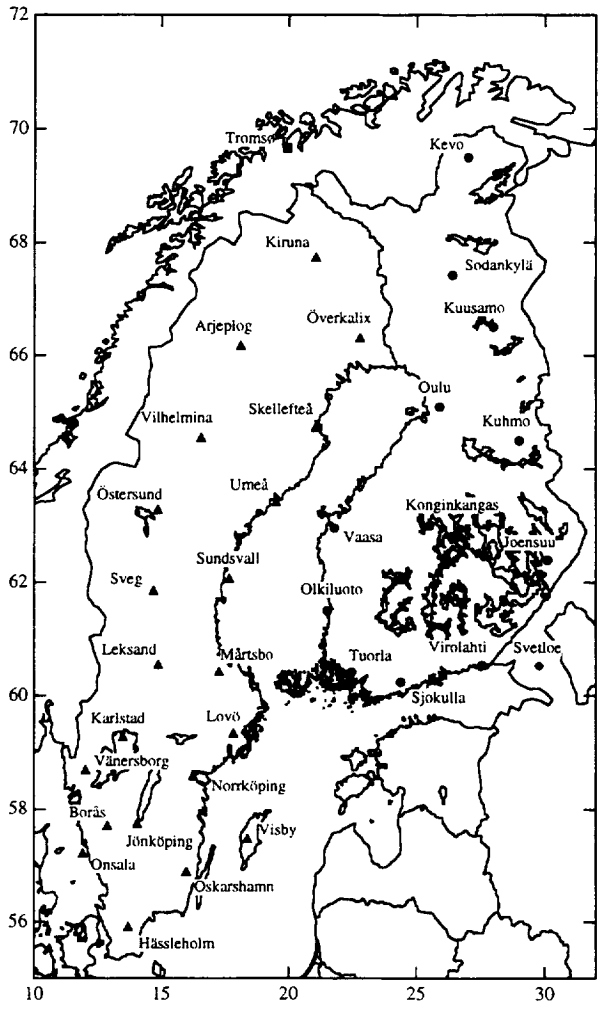

Figure 1. The BIFROST GPS networks.

The SWEPOS GPS network

The SWEPOS network (Figure 1) currently consists of 21 continuously operating GPS stations. The approximate coordinates of the stations, along with the history of operation, are given in Table 1. The requirement for site selection included access to unfractured bedrock and low horizon mask.

Care was taken to obtain similar signal receiving conditions at all sites. Nevertheless, some different types of GPS receiver/antenna combinations were used. SWEPOS employs 13 Rogue SNR-8000 (TurboRogue) and 20 Ashtech-Z12 GPS receivers. (Brand names are mentioned for identification purposes only. No endorsement of a manufacturer is implied.) At the time of the SWEPOS establishment, 15 TurboRogues were deployed. The TurboRogue receiver was then the only receiver able to provide full-wavelength phase observables when Anti-Spoofing (AS) was enabled. The Ashtech-Z12 receiver, introduced in 1994, also provides full-wavelength observables under all conditions and was added to provide Differential GPS (DGPS) corrections and Doppler observables for navigational applications. The Ashtech-Z12 is a 12-channel receiver whereas the TurboRogue possesses eight channels; the larger number of channels is required for reference stations in DGPS applications at high latitudes and is advantageous in static surveying application. Two receiver systems are operating in parallel at 12 sites. These receivers are connected to the same antenna using a power splitting device. The antenna pre-amplifier is powered by an external supply. Dorne-Margolin (DM) choke-ring antennas are used at all sites. However, they are of three different types, namely DM-B, DM-T, and DM-TA. The DM-TA and the DM-T have identical designs but were manufactured by different firms. The DM-B antenna is essentially identical to the other two except for the bottom of the ground-plane housing the pre-amplifier. The characteristics of this antenna (only used at station Onsala) are very similar to the other types [*Jaldehag et al.*, 1996b].

Each site (Figure 2) consists of a 3-m tall concrete pillar atop a concrete platform. At four sites a second pillar is available to serve as an alternate and as a platform for test measurements. The pillars are built on bedrock and the line of sight from the top to the GPS satellites is unblocked at elevation angles $> 10°$ and often lower. Each pillar is supported by four internal steel rods set 1 m into the underlying rock (Figure 2). Heating coils are wrapped around each concrete pillar and insulating material surrounds the wire-wrapped pillar. Electric power to the coils is controlled by a thermostat which keeps the pillar heated to a minimum of 15 °C. The pillars are not cooled. On the top of each pillar is a plate for the attachment of the GPS antenna (Figure 3). The antenna is protected from the environment by a fiberglass radome covering the antenna. The original radome, developed at Delft University, did not cover the whole top of the antenna and had a rather rough surface. This made it possible for snow to accumulate on top of the of the monument. *Jaldehag et al.* [1996a] showed that such snow accumulation could cause scattering and phase delay effects resulting in variations in the estimated vertical site positions of up to 10 cm. The radomes were replaced in February and June, 1995 in northern and southern Sweden,

respectively. The new radome, developed by the group at Onsala Space Observatory, is steeper and covers the whole top of the monument thereby preventing the accumulation of snow on top of and around the antenna. We also mounted a sharpened rod atop the radome to discourage the alighting of birds, the consequences of which seriously degraded signal-to-noise ratio.

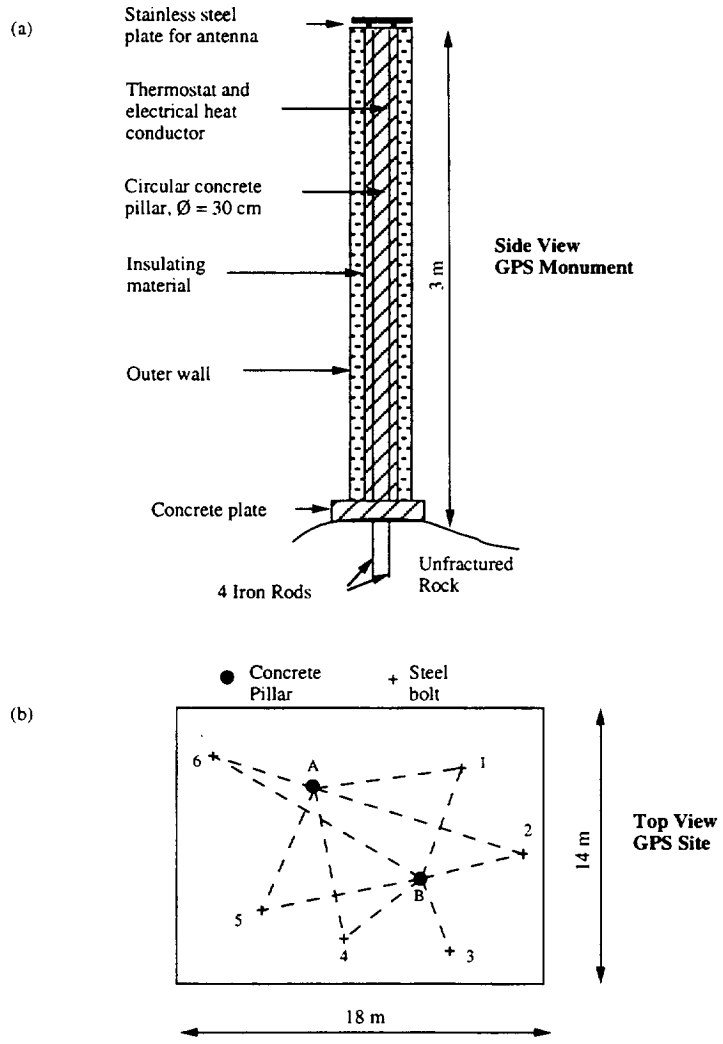

Figure 2. The SWEPOS Site sketch. (a) Pillar. (b) Local reference network.

The pillars at each site are surrounded by a network of steel pins, driven into the rock so that their tops protrude a few centimenters above the surface (Figure 2). This local network, covering an area of approximately 15 m $\times$ 15 m, is used to monitor the stability of the concrete pillars. The GPS antenna is removed from the pillar and replaced with a theodolite, which is used to measure the horizontal and vertical angles to the steel pins. Through resection the position of the pillar can be calculated. In this manner, the local position and orientation of the pillar may be monitored to

better than 1 mm. The first such measurements were obtained during summer 1993 and repeated annually except for the monument in Leksand where measurements are carried out monthly. The results of these measurements are described below.

Along with the monumentation described above, each site consists of a 3 m × 2 m hut housing the GPS receivers, backup batteries, computer, and modem. The extra power backup batteries will maintain operation of the station for 48 hr in case of external power failure. During the summer of 1994, lightning caused problems. Two telephone modems and four power backups were destroyed. New and better protected phone lines and power backup units have been deployed at the stations. The microcomputers (one 486 PC for each GPS receiver) have ~200 Mbyte of disk space available to enable four weeks of GPS data to be maintained on line as a backup. The large amount of electrical equipment in the huts has caused problems, especially during summer, with high temperatures. The latest addition to the instrumentation is a cooling system. Power and telephone communications are provided to the hut. In fact, several telephone lines are used to control the full system of two receivers and computers and retrieve data. All components can be remotely powered up and down in case of failure. Dedicated lines are used to transmit DGPS pseudorange corrections to a TV-tower in Stockholm at a rate of 0.5 Hz for all satellites above an elevation angle of 5°.

Every day, each GPS receiver is automatically contacted by a computer at the LMV in Gävle, Sweden. The GPS data acquired during the previous 24 hours at each site are then automatically downloaded. The observations are normally made with a 15 sec sample interval and a 5° elevation mask. For special applications epoch intervals down to 1 sec are possible. The size of the transferred binary compressed data file is approximately 2.5 Mbytes, and downloading proceeds at a rate of 19,200 baud. InterNet connections, which would significantly enhance communication to the sites in the network, are envisioned for the future. The data types provided for post-processing purposes are C/A-code pseudoranges, P-code pseudoranges on L1 and L2, carrier phase data on L1 and L2, doppler frequency and satellite ephemeris.

At the control center the data are converted to the Receiver INdepentent EXchange format (RINEX), and archived. Together with the actual data, a quality control indicator is available. The data is also transferred to OSO for independent archiving and extensive data analysis. This will be further described below.

The FinnNet GPS network

The FINNNET network currently consists of 12 sites (Figure 1) operating continuously. Sites were selected for sky visibility, location on bedrock (compromised only for the Sodankylä station, which has a 3 m deep concrete base), and proximity to a precise levelling line. Only later in the reconnaissance, the desirability of using an existing research station became more prominent.

Receivers used are all Ashtech Z-12 12 channel receivers with Dorne-Margolin choke ring antennas (types T or ASH), except Metsähovi, where a Turbo-Rogue (earlier a Mini-Rogue) is used, with a DM type B antenna.

At each site a 2.5 m high steel grid tower is used to mount the antenna with a horizontal triangular aluminum plate on the top. The antenna is attached to one corner of the plate. In three sites, slightly different towers were used: Metsähovi has a 22 m high tower girded by guy-wires, on which the height of the antenna platform is stabilized by an invar wire construction. In Oulu an 8 m high antenna tower was obtained by converting an existing radio astronomical instrument tower; it too is invar wire stabilized. Finally in Kevo, a 5 m high steel grid mast was used otherwise similar to the standard model. No attempt is made to stabilize the height of the grid masts; it was computed that the expansion/contraction cycle through the year amounts to some 2 mm, which was considered both acceptably small and "modelable" if needed.

In 1994, the attachment piece used up till then was replaced by the current, more robust model; also radomes ("snow hats") were mounted. These have proven less than satisfactory for their stated purpose, but we intend *not* to change our antenna mount solution any more; the snow accumulation problem we intend to cope with by simply eliminating data affected by it (The meteo stations planned to be installed at each site should be helpful for this). Furthermore, we intend (resources permitting) to perform *site calibrations* to precisely model the effects of both the attachment plate (multipath) and the radome (propagation effect). As the Swedish experience has shown, changes in antenna geometry, however justified technically, should be avoided at all cost if one want to obtain "strong" long term time series.

At those sites where no existing building could be used, 2 x 3 m huts were built. These are heated and thermostated and the receivers and modems are placed in a thermostated cabinet as well. Car batteries provide power backup.

Around the antenna masts, at least three reference bench marks have been struck. These are intended to be used for stability monitoring at regular intervals; however, such measurements have only been done in 1993 by tachymeter, and in 1994 by GPS. A repetition in the near future is foreseen. Also levelling connections to all stations have been made, except for Kuusamo, which is scheduled for this year.

The download of data happens automatically every 24 hours after midnight UTC from all the stations. The central computer is an ordinary PC. Ordinary dial-up telephone lines are used; these are not always reliable, but the receivers can store up to five days of data at a 30 second sampling rate, so there is time for repair. The data received are automatically rinexed and archived both on backup tape cassettes and writable CR-ROM. Automation of the processing routines is still in its infancy due to lack of personnel. Some quality control comes from the processing done at the NKG EUREF processing center at Onsala, Sweden.

Of the permanent stations of FINNNET, five were originally also used for the dissemination of RTCM DGPS corrections, in an agreement with the Finnish Broadcasting Company (YLE). Currently, only one station (Oulu) is being used for this, as YLE has progressively deployed their own receivers due to problems (reliability and cost) with the fixed telephone lines needed.

Data analysis and geodetic results

The dual-frequency GPS phase and pseudorange data were processed using the 2nd release of GIPSY software developed at Jet Propulsion Laboratory (JPL) [e.g., *Webb and Zumberge*, 1993]. Dual-frequency phase and pseudorange data from a single 24-hour period (boundary at 0 UT) acquired from all the sites in the network are analyzed simultaneously. Although the GPS data are recorded every 30 sec, at processing time data are decimated by a factor of 10 to achieve an effective sample rate of 300 sec; decimation is performed to maintain a manageable level of utilized disk space. For each 24-hour data set we estimated the usual set of parameters, including oscillator ("clock") corrections, site positions, atmospheric zenith delay parameters, and ambiguity parameters. Satellite orbit parameters were held fixed to the values distributed by the IGS based on a solution involving a global network of GPS sites. Temporal variations in the clock and atmosphere parameters are modeled as independent random walks. We adopted a minimum elevation angle of 15° for all stations.

We adopted the value of 10 mm for the uncertainties for the phase measurements at each frequency. The instrumental uncertainties for such measurements are much smaller, perhaps 2–3 mm. However, experience within the GPS community has shown that the scatter of the time series is greater than the theoretical value based on instrumental noise only. The increase in the scatter above the predicted value can of course be attributed to unmodeled phase variations, which may or may not have a white noise (or nearly white noise) nature. In the next section, we discuss a number of errors which might be contributing to this increased scatter, and we investigate the spectral characteristics of the site position variations. It is important to remember throughout the paper, though, that the uncertainties for the estimated parameters, including site position and therefore velocity and geophysical parameters, are approximations.

Data processing utilizes a "no-fiducial" technique wherein station coordinates have only weak a priori constraints [*Heflin et al.*, 1992]. The seven parameters describing the transformation to the ITRF94 reference frame are estimated by means of a least squares fit using the estimated positions for some of the stations in the global network.

The results presented in the following sections were achieved without fixing to integer values the estimated phase biases, since the software cannot yet handle automatically such an extensive data set. Independent tests with a smaller data set (SWEPOS stations only) have shown that "bias fixing" leads to a decrease in the formal errors of about 20–30%. However, no significant change in the day-to-day repeatability was observed.

The daily analyses yield time series of three-dimensional position in the ITRF94 reference frame. The corrections for plate motion effect the horizontal components of velocity only.

Several of the time series for sites of the Swepos network exhibit one or more "jumps." We do not believe that these jumps represent motions of the GPS antenna. On most of the occasions on which jumps occurred, the GPS antenna was not moved. The GPS antennas were removed and replaced occasionally to perform the local site

surveys described above. The GPS antenna with a threaded hole is positioned by means of a standard 5/8" surveyor's bolt which is attached to a metal plate which has been permanently set into the concrete at the top of the pillar. The GPS antenna is screwed onto the bolt until it refuses to rotate. When the antennas are removed and replaced, the orientation of the antenna is checked to insure that it is the same as before removal. Given that the surveyor's bolt has 5 threads per inch, a rather large orientation error of 45° would lead to a vertical displacement of only 0.6 mm, and to no horizontal displacement. The observed "jumps," on the other hand, can be at the 10 mm level, and, as we mentioned above, many occur at times when the antenna was not moved.

A likely explanation for these jumps is that very small differences in antenna orientation lead to changes in phase errors because of electromagnetic coupling [*Elósegui et al.*, 1995; *Jaldehag et al.*, 1996b] and antenna phase center variations [*Schupler et al.*, 1994]. Both these sources of error are potentially elevation- and azimuth-angle dependent, and in the case of the former the position relative to the pillar and metal plate is critical. If one imagines that the phase errors induced by these two phenomena can be represented as a series of spherical harmonics, with angular arguments of azimuth and elevation angles, then the contribution from the $\ell = 1$ term is indistinguishable from the contribution to phase variations from a site position offset.

As an ad hoc treatment for these errors, we have simply estimated three-dimensional offsets in position on the epochs at which radomes were changed, the GPS antennas removed and replaced, or the antenna rotated. The site velocity was assumed to be constant for the entire experiment. This ad hoc procedure is not very satisfying, since the existence of the "jumps" is an indication of an error source which could conceivably have a temporal variation and therefore could effect the estimate of the rate.

Estimated site positions and velocities in the ITRF94 frame are presented in Table 1. We have limited the analysis to sites which have a span of data of 2 yr or longer.

Correlation analysis

Formally, the correlation between errors in the estimates of relative position at different sites have very low correlations. The low values result, in part, because of our method for determining the reference frame in our "standard" solutions. By taking the satellite orbital parameters as being known exactly, and by using a regional network of GPS sites to realize, day-by-day, a pre-determined reference frame (ITRF94), the determinations of site position, from the least-squares point of view, are independent.

In reality, reference frame and orbit errors could be significant, and hence we might expect non-zero correlations among determinations of relative position within our network. Other sources of error may also be more or less correlated from site to site, such as signal scattering caused by the antenna mount structure, atmosphere, antenna phase patterns, and atmosphere and ocean loading.

Table 1. Site coordinates, velocities, and uncertainties.

Site	Latitude			Longitude			Velocity, mm yr^{-1}		
							North	East	Up
Arjeplog	66	19	4.85779	18	07	29.50562	14.4 ± 0.2	16.1 ± 0.3	8.3 ± 0.9
Hässleholm	56	05	31.97937	13	43	5.06584	13.9 ± 0.2	21.3 ± 0.3	0.6 ± 0.8
Jönköping	57	44	43.69904	14	03	34.58359	13.8 ± 0.1	17.7 ± 0.2	3.0 ± 0.6
Karlstad	59	26	38.46954	13	30	20.24231	14.5 ± 0.2	18.8 ± 0.3	6.6 ± 0.8
Kiruna	67	52	39.25598	21	03	36.84952	13.5 ± 0.2	18.9 ± 0.2	5.4 ± 0.8
Leksand	60	43	19.72229	14	52	37.22008	14.3 ± 0.2	15.9 ± 0.3	8.9 ± 0.7
Mårtsbo	60	35	42.51251	17	15	30.68619	12.9 ± 0.2	18.9 ± 0.3	10.3 ± 0.8
Onsala	57	23	43.07281	11	55	31.85120	13.7 ± 0.1	17.9 ± 0.2	2.8 ± 0.5
Oskarshamn	57	03	56.30219	15	59	48.50555	13.8 ± 0.3	20.0 ± 0.6	2.4 ± 1.5
Skellefteå	64	52	45.10620	21	02	53.83118	13.9 ± 0.2	20.3 ± 0.4	15.8 ± 1.2
Sundsvall	62	13	56.91101	17	39	35.58746	13.7 ± 0.2	18.1 ± 0.3	10.8 ± 0.8
Sveg	62	01	2.69073	14	42	0.03708	14.6 ± 0.2	17.0 ± 0.3	10.0 ± 0.8
Umeå	63	34	41.29120	19	30	34.53827	12.6 ± 0.2	18.4 ± 0.3	13.3 ± 0.7
Vilhelmina	64	41	52.24365	16	33	35.74402	14.7 ± 0.2	16.4 ± 0.3	8.9 ± 0.8
Visby	57	39	13.93066	18	22	2.32819	12.7 ± 0.1	19.8 ± 0.2	2.1 ± 0.6
Vänersborg	58	41	35.25604	12	02	6.00288	14.6 ± 0.2	17.5 ± 0.4	4.2 ± 1.2
Östersund	63	26	34.04755	14	51	29.03618	14.5 ± 0.2	17.0 ± 0.3	9.0 ± 0.8
KOSG	52	10	42.32941	5	48	34.70901	15.4 ± 0.1	18.7 ± 0.1	1.4 ± 0.3
WETB	49	08	39.20013	12	52	44.04190	14.9 ± 0.1	22.0 ± 0.1	-0.3 ± 0.3
Tromsø	69	39	45.90088	18	56	17.97318	14.9 ± 0.1	15.5 ± 0.1	1.2 ± 0.3
HERS	50	52	2.32819	0	20	10.56850	15.7 ± 0.1	18.1 ± 0.1	-0.2 ± 0.3
MADR	40	25	44.97986	−4	14	58.78120	15.9 ± 0.1	19.9 ± 0.1	0.2 ± 0.2
MATE	40	38	56.86066	16	42	16.04279	18.3 ± 0.1	23.2 ± 0.2	0.5 ± 0.4
Metsahovi	60	13	2.89948	24	23	43.14148	11.4 ± 0.1	19.3 ± 0.1	5.4 ± 0.3
Ny Ålesund	78	55	46.49048	11	51	54.29787	14.6 ± 0.1	12.4 ± 0.1	3.7 ± 0.3
SAAR	67	51	26.47156	20	58	6.39450	13.5 ± 0.1	16.6 ± 0.1	3.7 ± 0.4
Lovö	59	20	16.00800	17	49	44.12018	13.2 ± 0.3	19.7 ± 0.6	3.0 ± 2.0
Norrköping	58	35	24.82452	16	14	46.96747	12.1 ± 0.3	19.7 ± 0.6	7.2 ± 1.5
Överkalix	66	19	4.28101	22	46	24.13467	14.9 ± 0.6	17.1 ± 0.9	9.6 ± 2.8
Joensuu	62	23	28.22754	30	05	46.15860	12.8 ± 0.3	23.3 ± 0.5	2.0 ± 2.9
Sodankylä	67	25	14.73999	26	23	20.57144	12.6 ± 0.7	17.3 ± 1.2	4.5 ± 6.1
Tuorla	60	24	57.05200	23	26	36.32034	13.1 ± 0.3	21.5 ± 0.5	5.9 ± 1.3
Vaasa	62	27	40.29510	21	46	14.28131	13.3 ± 0.3	18.7 ± 0.6	11.0 ± 1.5
Virolahti	60	32	19.67743	27	33	17.98050	12.0 ± 0.3	23.8 ± 0.5	-2.9 ± 1.3
Olkiluoto	61	14	22.75635	21	28	21.63116	12.3 ± 0.4	22.4 ± 0.6	10.4 ± 1.8
Oulu	65	05	11.48987	25	53	34.52408	13.5 ± 0.4	19.3 ± 0.6	5.4 ± 1.7
Riga	56	56	55.03143	24	03	31.57608	12.0 ± 0.4	20.8 ± 0.7	0.0 ± 0.0

In lieu of a site-by-site correlation analysis, we have performed a more general principal component, or empirical orthogonal function (EOF), analysis. An EOF analysis is used to assess temporal and spatial coherences of time series. As applied to our problem, the time series for a given site component $x_p(t)$ for the pth site is first reduced to a detrended unit variance time series N_{pq}:

$$N_{pq} = \frac{x_p(t_q) - \alpha_p - \beta_p(t - t_\circ)}{\sigma_p} \tag{1}$$

where α_p and β_p are the parameters of the best-fit line and σ_p the RMS residual for the series of position determinations for the pth site. (The term x will take on the values of the north, east, or vertical component of site position.) N is thus a matrix of normalized coordinate values. The following matrices are then formed:

$$A = N^T N/(n_s n_t) \qquad B = NN^T/(n_s n_t) \tag{2}$$

where n_s is the number of sites, and n_t is the number of epochs (see below). The square symmetric matrices A and B are positive definite; A is of order n_t and B is of order n_s. It is straightforward to show that their first n eigenvalues are identical, where n is the smaller of n_s and n_t. Let us label these eigenvalues $\lambda^{(1)}$, $\lambda^{(2)}$, ..., $\lambda^{(n)}$, in order of decreasing eigenvalue. If $T^{(k)}$ is the eigenvector of A associated with the kth eigenvalue, and $S^{(k)}$ is the corresponding eigenvector for B, then we may write the matrix N as the series

$$N_{pq} = \sum_{k=1}^{n} [n_s n_t \lambda^{(k)}]^{1/2} \, S_p^{(k)} T_q^{(k)} \tag{3}$$

If high correlations exist among the time series from the different sites, then one finds that lowest-k eigenvalues are relatively large. The normalization (1)–(2) of the covariance matrices insures that the eigenvectors are orthonormal, and that the sum-square of the eigenvalues is unity. Thus, λ_k is a measure of the variance which is "explained by" the kth term of the series (3). An estimate of N_{pq}, for example, may be obtained using only the first eigenvectors:

$$N_{pq}^{(1)} = [n_s n_t \lambda^{(1)}]^{1/2} \, S_p^{(1)} T_q^{(1)} \tag{4}$$

The EOF analysis is related to the correlation analysis in the following way. Given the first eigenvector approximation (4), the correlation R_{pq} between time series for the pth and qth sites is

$$R_{pq} = n_s \lambda^{(1)} S_p^{(1)} S_q^{(1)} + (1 - n_s \lambda^{(1)} S_p^{(1)} S_q^{(1)}) \delta_{pq} \tag{5}$$

where δ_{pq} is the Kronecker delta. A high spatial correlation will give $S_p^{(1)} = S_q^{(1)} = 1/\sqrt{n_s}$, in which case (5) becomes

$$R_{pq} = \lambda^{(1)} + (1 - \lambda^{(1)})\delta_{pq} \tag{6}$$

Thus, the first eigenvalue is the correlation of the time series for two different sites. The variance $\hat{\sigma}_p^2$ of the residual time series, i.e., the observed time series minus the first eigenvector approximation (4), is

$$\hat{\sigma}_p^2 = \sigma_p^2(1 - \lambda^{(1)}) \tag{7}$$

For our EOF analysis, we chose to use the nine sites with the longest timespan and the fewest gaps. We chose to use the determinations from the first ~1.5 yr, and sampled the data set every eight days to enable reasonably rapid calculation of the eigenvectors. (The time to compute the eigenvectors increases as the cube of the matrix dimension.) The resulting data set had $n_t = 161$. The spatial and temporal eigenvectors from the EOF analysis of the vertical components for $k = 1$–3 are shown in Figure 3. The first spatial eigenvector (Figure 3b) is fairly constant, indicating a high spatial coherence. The second spatial eigenvector seems to indicate a north-south anticorrelation, and the third spatial eigenvector indicates an anticorrelation between mainly Onsala and Metshahovi, which is the largest east-west baseline. Visby is the only other site whose component of the third spatial eigenvector is greater than 0.2; Visby lies directly between Onsala and Mestähovi.

The EOF analyses for each of the components indicates that the correlation among the time series of different sites is ~50%. In absolute terms, a constant correlation means that the variation (in an RMS sense) of the correlated "error" scales with the variation of the uncorrelated part. One typically finds that the RMS variability for each of the three components of site position differs due to different satellite constellation geometry as viewed from the site: north has the smallest RMS variability (typically 2–3 mm for our sites); east has a slightly larger value (typically 4–6 mm); and vertical the greatest (10–15 mm). Thus, the EOF analysis indicates that the error source(s) associated with the first eigenvector has standard deviations of 1–2 mm (north), 3–4 mm (east), and 7–11 mm (vertical).

This scaling implies to us that the main effect is one of reference frame, for the realization of the reference frame, through the constraints tying the positions of the regional GPS network to their ITRF94 values, should have an accuracy which is commensurate with the errors in determination of the site position. Further evidence for this conclusion comes from the analysis of the second and third spatial eigenvectors, which indicate anticorrelations directed along two orthogonal axes. If the first eigenmode represents a translation of the network in the instantaneously realized ITRF94, the second and third eigenmodes would then represent a tilting of the network. Since we expect that the network is neither translating nor tilting instantaneously, the errors are presumably in the realization of the reference frame, as transmitted through the orbital parameters.

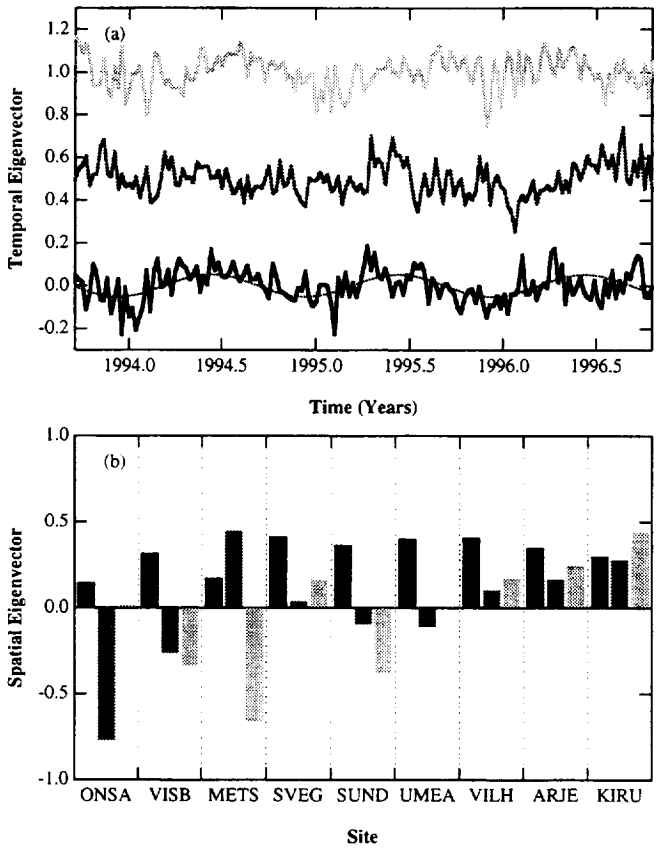

Figure 3. First three (a) temporal and (b) spatial eigenvectors from the EOF analysis. Color code: Black, $k = 1$ mode; dark gray, $k = 2$; light gray, $k = 3$. The $k = 2$ temporal eigenvector has been offset by +0.5 and the $k = 3$ by +1.0 for clarity.

Monument stability

As described in the section describing the GPS networks, we monitor the relative position of the pillar reference point within a local (10–15 m area) network of reference pins. Based on the RMS analysis of all the data, the standard deviation of a single measurement is 0.2 mm for the north, 0.3 mm for the east, and 0.4 mm for the vertical. However, there are several occasions when repeated measurements are obtained in a single day. The five repeated measurements from the Leksand site, for instance yield RMS differences of 0.01 mm for north, 0.04 for east, and 0.06 mm for vertical. The single repeated measurement for Kiruna, on the other hand, yields an RMS difference (based on two measurements) of 0.2 (north), 0.3 (east), and 0.1 mm (up), roughly consistent with the same statistics for the single repeated measurement for the Överkalix site: 0.03 (north), 0.1 (east), and 0.1 mm (up); and for the Norrköping site: 0.1 (north), 0.1 (east), and 0.1 mm (up). If we combine the Kiruna, Överkalix, and Norrköping repeat measurements, we find an RMS error of 0.10 (north), 0.18 (east), and 0.10 (north). We will therefore adopt 0.13 mm as our uncertainty in each

of the components. We have no explanation as to why the differences in the repeated Leksand measurements are so small relative to these values. Eliminating the multiple measurements by replacing them with their average, the overall RMS variations for all

applications of space geodetic measurements in Fennoscandia, in *Proceedings of the International Workshop for Reference Frame Establishment and Technical Development*, January 18–21, Tokyo, 248–255, 1993.

2. Mitrovica, J. X., J. L. Davis, and I. I. Shapiro, Constraining proposed combinations of ice history and earth rheology using VLBI-determined baseline length rates in North America, *Geophys. Res. Lett.*, *20*, 2387–2390, 1993.

3. Mitrovica, J. X., J. L. Davis, and I. I. Shapiro, A spectral formalism for computing three-dimensional deformations due to surface loads, 1. Theory, *J. Geophys. Res.*, *99*, 7057–7074, 1994.

4. Mitrovica, J. X., J. L. Davis, and I. I. Shapiro, A spectral formalism for computing three-dimensional deformations due to surface loads, 2. Present-day glacial isostatic adjustment, *J. Geophys. Res.*, *99*, 7075–7102, 1994.

5. Mitrovica, J. X., J. L. Davis, P.M. Mathews, and I.I. Shapiro, Determination of tidal h Love number parameters in the diurnal band using an extensive VLBI data set, *Geophys. Res. Lett.*, *21*, 705–708, 1994.

6. Mitrovica, J. X., and J. L. Davis, Some comments on the 3-D impulse response of a Maxwell viscoelastic Earth, *Geophys. J. Int.*, *120*, 227–234, 1995.

7. Elósegui, P., J. L. Davis, R. T. K. Jaldehag, J. M. Johansson, A. E. Niell, and I. I. Shapiro, Geodesy using the Global Positioning System: The effects of signal scattering on estimates of site position, *J. Geophys. Res.*, *100*, 9921–9934, 1995.

8. Mitrovica, J. X., and J. L. Davis, Sea level change far from the Late Pleistocene ice sheets: Implications for recent analyses of tide gauge records, *Geophys. Res. Lett.*, *22*, 2529–2532, 1995.

9. Mitrovica, J. X., and J. L. Davis, The influence of a finite glaciation phase on predictions of post-glacial isostatic adjustment, *Earth Planet. Sci. Lett.*, *136*, 343–361, 1995.

10. Davis, J. L., and J. X. Mitrovica, Glacial isostatic adjustment and the anomalous tide gauge record of eastern North America, *Nature*, *379*, 331–333, 1996.

11. Jaldehag, R. T. K., J. M. Johansson, P. Elósegui, J. L. Davis, Geodesy using the Swedish permanent GPS network: Effects of snow accumulation on estimates

12. Elósegui, P., J. L. Davis, J. M. Johansson, and I. I. Shapiro, Detection of transient motions with the Global Positioning System, *J. Geophys. Res.*, *101*, 11,249–11,261, 1996.

13. Jaldehag, R. T. K., J. M. Johansson, B. O. Rönnäng, P. Elósegui, and J. L. Davis, and I. I. Shapiro, Geodesy using the Swedish permanent GPS network: Effects of signal scattering on estimates of relative site positions, *J. Geophys. Res.*, *101*, 17,841–17,860, 1996.

14. BIFROST Project Members, GPS measurements to constrain geodynamic processes in Fennoscandia, *Eos Trans. AGU*, *77*, pp. 337 & 341, 1996.

15. Elgered, G., J. M. Johansson, B. O. Rönnäng, and J. L. Davis, Measuring regional atmospheric water vapor using GPS, *Geophys. Res. Lett.*, *24*, 2663–2666, 1997.

16. Davis, J. L., and G. Elgered, The spatio-temporal structure of GPS water-vapor determinations, *Phys. Chem. Earth*, in press, 1998.